Diagnosis of Early-Stage Glaucoma by Grid-Wise Macular Inner Retinal Layer Thickness Measurement and Effect of Compensation of Disc-Fovea Inclination

Chihiro Mayama,[1] Hitomi Saito,[1,2] Hiroyo Hirasawa,[1] Atsuo Tomidokoro,[1] Makoto Araie,[1,2] Aiko Iwase,[3] Shinji Ohkubo,[4] Kazuhisa Sugiyama,[4] Masanori Hangai,[5] and Nagahisa Yoshimura[5]

[1]Department of Ophthalmology, the University of Tokyo Graduate School of Medicine, Tokyo, Japan
[2]Kanto Central Hospital, Tokyo, Japan
[3]Tajimi Iwase Eye Clinic, Tajimi, Japan
[4]Department of Ophthalmology & Visual Science, Kanazawa University Graduate School of Medical Science, Kanazawa, Japan
[5]Department of Ophthalmology and Visual Sciences, Kyoto University Graduate School of Medicine, Kyoto, Japan

Correspondence: Chihiro Mayama, Department of Ophthalmology, the University of Tokyo Graduate School of Medicine, 7-3-1 Hongo, Bunkyo-ku, Tokyo 113-8655, Japan; cmayama-tky@umin.ac.jp.

Submitted: May 2, 2015
Accepted: July 16, 2015

Citation: Mayama C, Saito H, Hirasawa H, et al. Diagnosis of early-stage glaucoma by grid-wise macular inner retinal layer thickness measurement and effect of compensation of disc-fovea inclination. *Invest Ophthalmol Vis Sci*. 2015;56:5681–5690. DOI:10.1167/iovs.15-17208

Purpose. To evaluate grid-wise analyses of macular inner retinal layer thicknesses and effect of compensation of disc-fovea inclination for diagnosing early-stage glaucoma.

Methods. Spectral-domain optical coherence tomography measurements over a 6.0 × 6.0-mm macular area were prospectively obtained in 104 eyes of 104 patients with early-stage glaucoma with a mean deviation of −1.8 ± 1.9 dB and 104 eyes of 104 age- and refraction-matched normal subjects. Macular retinal nerve fiber layer (mRNFL), ganglion cell-inner plexiform layer (GCIPL) combined, and ganglion cell complex (GCC) thickness of the entire area and each subdivided macular grid were determined to compare diagnostic capability for glaucoma using receiver operating characteristic curves and various normal cutoff values for each layer thickness and number of grids flagged as abnormal. Diagnostic capability was then compared with that of circumpapillary RNFL (cpRNFL) measurements. Effects of compensation of inclination of disc-fovea line by reconfiguration of the macular grid were also studied.

Results. Macular inner retinal layer analyses using 8 × 8 grids generally yielded higher diagnostic capability. Only the 8 × 8 grid GCC analyses using the various normal cutoff values yielded a sensitivity ≥ 0.90 with specificity ≥ 0.95 under several conditions in discriminating the glaucoma eyes. In glaucoma and normal eyes with both reliable cpRNFL and macular measurements, the best sensitivity/specificity were 0.98/0.95 for the 8 × 8 grid-mRNFL analysis and 0.93/0.96 for the 8 × 8 grid GCC analysis using various normal cutoff values, which were better than that (0.78/0.95) for clock-hour cpRNFL analysis ($P = 0.001$). Compensation of the disc-fovea inclination did not improve the diagnostic capability.

Conclusions. Grid-wise analysis of macular GCC—especially using 8 × 8 grids and normative data-based cutoff values—was very useful for diagnosing early-stage glaucoma, though compensation of the disc-fovea inclination had little effect.

Keywords: glaucoma, optical coherence tomography, inner retinal layers, grid

Optical coherence tomography (OCT) effectively detects glaucomatous optic neuropathy with early visual field damage.[1–7] Optical coherence tomography–based glaucoma diagnosis is based mainly on analyzing the circumpapillary retinal nerve fiber layer (cpRNFL) thickness and/or optic disc morphology.[8–12] Major retinal vessels in the circumpapillary area, however, may limit detection of early glaucomatous changes. Moreover, reliable and automatic determination of the anatomical disc margin or Bruch membrane's opening, which is an important benchmark for cpRNFL measurements, may be difficult.[13] On the other hand, analysis of detailed structure-function relationships is possible in the macular area, which contains ≥50% of the whole retinal ganglion cells.[14] Measurements of OCT are less affected by retinal vessels and automatic determination of the fovea as the center of the analysis area is technically easier in the macular area without manifest pathological changes.

Current spectral-domain (SD)-OCT devices are equipped with software that provides automatic segmentation and thickness measurements of macular inner retinal layers, including the macular retinal nerve fiber layer (mRNFL), ganglion cell layer (GCL) + inner plexiform layer (GCIPL), and the mRNFL + GCIPL (ganglion cell complex, GCC).[15–17] Several SD-OCT studies report significant decreases in the thicknesses of these layers in eyes with early-stage glaucoma,[18–20] even in those lacking manifest visual field defects (VFD) in standard static automated perimetry.[21,22]

The diagnostic capability of macular GCIPL or GCC has been studied based on the thickness of the layers over the whole macula,[19,20,23] hemifield, or sectorial macular area,[24–26] and macular GCIPL or GCC measurements have similar glaucoma

Table 1. Characteristics of the Subjects

Glaucomatous Damage	Normal	Early-Stage
Number of subjects, eyes	104	104
Women/men*	55/49	71/33
Age, y	57.6 ± 11.0	58.2 ± 10.2
Refraction, D	−1.04 ± 1.28	−1.41 ± 2.12
Mean deviation, dB†	−0.15 ± 1.17	−1.80 ± 1.93

Refraction indicates spherical equivalent of the subject eye. Mean deviation indicates mean deviation of a central 24-2 test program of Humphrey Field Analyzer. Intergroup difference was significant at $^*P = 0.023$, χ^2-test and $\dagger P < 0.001$, Mann-Whitney U test.

detection capabilities.[23,25–28] Visual field defects were identified using the central 10-2 test program in a significant portion of eyes with normal visual field (VF) test results with a central 24-2 test program (Humphrey Field Analyzer [HFA], Carl Zeiss Meditec, Dublin, CA, USA).[29] Thus, subdividing the macula further, as in the central 10-2 visual field test, may yield better diagnostic capability for detecting early glaucomatous abnormalities. A recent study reported that cluster analysis of mRNFL or GCIPL thickness divided into 10×10 grids over the macula produced better sensitivity than mean thickness of these structures over the whole or hemiretinal macula.[28] Moreover, compensation for the inclination of disc center-fovea line, that is, the difference between the anatomical horizontal line and the horizontal line on the fundus photograph, might increase the diagnostic capability of SD-OCT circumpapillary or macular inner layer parameters.[13]

We systematically investigated the diagnostic capability of analytical methods by further subdividing the macula into grid-wise square areas in eyes with early-stage glaucoma. Effects of compensation of the inclination of disc-fovea line on the diagnosis were also studied.

Materials and Methods

Subjects

Data for normal subjects and open-angle glaucoma (OAG) patients were prospectively acquired from four institutes in Japan using the same selection criteria: the University of Tokyo (Tokyo, Japan), Kanazawa University (Kanazawa, Japan), Kyoto University (Kyoto, Japan), and Tajimi Municipal Hospital (Gifu, Japan). The study protocol was approved by each institution's institutional review board and adhered to the tenets of the Declaration of Helsinki. Written informed consent was obtained from each subject after explanation of the study protocol.

We recruited self-reported healthy volunteers $\geq$ 20 years of age. The following ocular examinations were performed at the first visit: refraction and corneal curvature (ARK-900; NIDEK, Tokyo, Japan), best-corrected visual acuity, axial length (IOL Master; Carl Zeiss Meditec, Inc.), biomicroscopy, intraocular pressure (IOP, Goldmann applanation tonometry), dilated funduscopy, and VF test (HFA 24-2 SITA standard program). Exclusion criteria were: contraindication to pupil dilation; IOP $\geq$22 mm Hg; best-corrected visual acuity $\leq$20/25; refractive error $\leq$ –6.0 diopters (D) or $\geq$ +3.0 D; unreliable HFA results (fixation loss, false-positive, or false-negative $>$ 20%); VFDs suggestive of glaucoma according to Anderson and Patella's criteria[30]; history of intraocular or refractive surgery or ocular or systemic diseases that could affect the OCT results, including cataract or macular degeneration; and optic nerve or retinal abnormalities.

Open-angle glaucoma patients fulfilling the following criteria were consecutively enrolled in each institute and underwent the same examinations as above. Inclusion criteria were: 1) accustomed to VF testing and producing reliable and reproducible VF test results with mean deviation (MD) of $>$–6.0 dB; 2) apparent glaucomatous changes in the optic disc with or without apparent RNFL defects confirmed by glaucoma specialists (MA, AI) according to stereo-fundus photographs and digitally constructed red-free photographs. Apparent glaucomatous changes in the optic disc referred to here are a rim notch with a remaining rim $\leq$ 0.1 of the disc diameter or a vertical cup-to-disc ratio $>$ 0.7 in one eye with that of the fellow eye smaller by $\geq$0.2 not explained by differences in disc size. Glaucomatous VFDs were not a concern when apparent disc findings and/or RNFL defects were wider than the major retinal vessel diameter at the disc margin; 3) eyes with refractive error $>$ –6.0 D and $<$ 3.0 D; and 4) no history of any other ocular pathologic changes that could affect the results of HFA or OCT examinations, including incisional intraocular surgeries or refractive surgeries. The Humphrey field analyzer 24-2 SITA standard program results were obtained within 3 months of the OCT examination, and glaucomatous VFDs were defined by 1) a cluster of $\geq$3 points in the pattern deviation plot in a single hemifield (superior/inferior) with $P < 0.05$, one of which must have been $P < 0.01$, 2) glaucoma hemifield test result outside of normal limits, or 3) abnormal pattern standard deviation with $P < 0.05$.[30] If both eyes of a subject were eligible, we included the eye with better data quality in the SD-OCT examination.

Finally, macular OCT images fulfilling the criteria described below were obtained in 104 early-stage OAG eyes of 104/181 initially enrolled OAG patients. From all normal subjects meeting the inclusion criteria, we selected those matched to glaucoma patients in terms of age and refraction (within 1 year of age and 1 D of spherical equivalent). Thus, 104 age- and refraction-matched normal eyes of 104/261 normal subjects were selected (Table 1).

OCT Measurements

Optimal coherence tomography scanning was performed using a three-dimensional (3D) OCT-1000 Mark II (Topcon, Inc., Tokyo, Japan) after pupillary dilation with 1% tropicamide. Spectral-domain OCT datasets were obtained with the raster-scan protocol in which data were obtained in 6.0×6.0-mm^2 areas (128 scan lines each comprised of 512 A-scans) centered on the fixation point within approximately 2.5 seconds. The magnification effect was corrected according to the manufacturer-provided formula[31,32] based on refractive error, corneal radius, and axial length. Registration of fundus photographs and OCT images was automatically confirmed using an OCT projection image and localization of major retinal vessels. Measurements in the macula were repeated three times at several second intervals.

A similar raster scan was performed centered on the optic disc, and repeated three times. The disc center was determined as the barycenter of the closed spline curve fitted to seven manually determined points on the disc edge in a simultaneously obtained color fundus photograph by the non-mydriatic fundus camera function of the instrument used, and extrapolated in all OCT images thereafter.

Data influenced by eye movements, involuntary blinking, or saccade, indicated by breaks or shifting of the images or a straight line across the image, or those with a quality factor $<$ 60% were discarded. Data with the best quality factor (given by the SD-OCT apparatus based on signal intensity) were adopted.

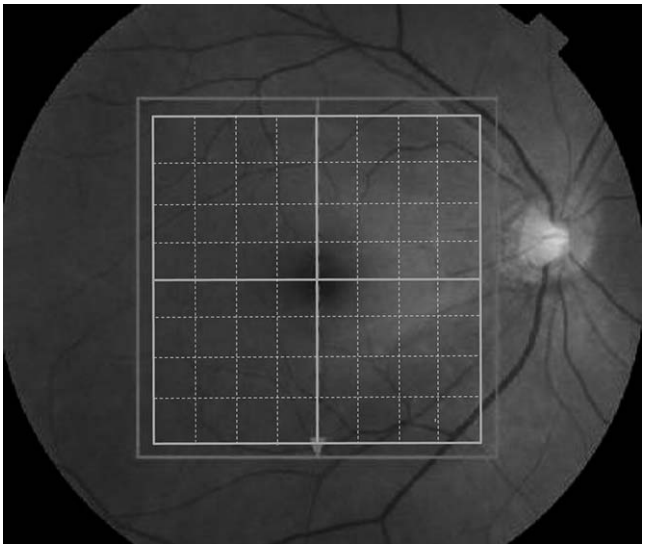

FIGURE 1. An example of location pattern of 8 × 8 grids in the 5.5 × 5.5-mm analysis area in a sample eye (right eye with early-stage glaucoma).

Analysis of the OCT Data

In the macula, the fovea was automatically identified in the OCT image as the sampling point with the thinnest retinal thickness adjacent to the fixation point, and the 5.5 × 5.5-mm square area centered on the fovea was analyzed. Eyes for which the analysis area exceeded the edge of the 6.0 × 6.0-mm data acquisition area were excluded. Macular retinal nerve fiber layer and GCIPL were automatically segmented[16] and confirmed on all B-scan images by an experienced examiner (MH), and the layer thicknesses were determined at each sampling point. The 5.5 × 5.5-mm analysis area was divided into upper and lower hemiretina, 4 × 4, or 8 × 8 grids where the thicknesses of mRNFL, GCIPL, and GCC (mRNFL + GCIPL) were calculated as the mean thickness over all sampling point within each grid (Fig. 1).

Diagnostic Capability of mRNFL, GCIPL, and GCC

Receiver operating characteristic (ROC) curve analyses were performed to study the capability of mRNFL, GCIPL, and GCC to discriminate current glaucoma eyes from age- and refraction-matched normal eyes. The area under the ROC curve (AUC) was calculated for the whole analysis area, upper or lower hemiretina, or each of the 4 × 4 and 8 × 8 grids with varied cutoff levels of mRNFL, GCIPL, or GCC thickness. The area or grid with the greatest AUC was determined and sensitivity was calculated when specificity was 0.95 in the ROC curve. Then sensitivity/specificity of glaucoma detection was calculated by normative data-based cutoff values of mRNFL, GCIPL, or GCC thickness using single or contiguous multiple grids. An eye was diagnosed with glaucoma if the thickness was lower than the 0.5th, 1st, 2.5th, 5th, or 10th percentile of the normative database in the whole macula, one or both of the hemiretinas, or one or multiple contiguous grids in 4 × 4 or 8 × 8 grids in the same hemiretina. The Japanese age-specific normative database was established in another group of 272 normal eyes.[33,34] The central four grids adjacent to the fovea were excluded from the analyses of the 8 × 8 grids of the mRNFL. The procedure of analyses is illustrated in Figure 2.

Comparison of cpRNFL and Macular Inner Retinal Layer Thickness Measurements

Results for mRNFL, GCIPL, or GCC were compared with those for cpRNFL in eyes of the same cohort of the subjects where eligible data for both macular and circumpapillary areas were obtained. Thickness of RNFL along a 3.4-mm diameter circle centered on the optic disc center was obtained from the raster scan data and averaged along the whole circumference or in sectors, each accounting for upper or lower 180°, 90°, or 30°, and the sector with the greatest AUC was determined and sensitivity was calculated when specificity was 0.95 in the ROC curve. Then the sensitivity/specificity was determined based on the number of abnormal sectors and normal data-based cutoff values (percentiles: 0.5th, 1st, 2.5th, 5th, or 10th percentile) of cpRNFL thickness established in a separate group of normal eyes[35] similar to the analysis in the macular area.

Effects of the Compensation of Inclination of Disc-Fovea Line on Grid-Wise Analyses of Macular Inner Retinal Layer Thicknesses

The optic disc center and fovea were determined on the fundus photograph as described above and we calculated the angle between the line connecting those two points and the horizontal line, and positive angle indicates fovea is located below the horizontal line (Fig. 3a). The analysis area was then changed from 5.5 × 5.5 mm to 4.8 × 4.8 mm, so that the most peripheral grid locating at a corner of the square did not exceed the data acquisition area (6.0 × 6.0 mm), and grids were reconfigured in parallel with the line connecting the optic disc center and fovea (Fig. 3b). When any of the most peripheral grids exceeded the data acquisition area (6.0 × 6.0 mm), the eye was excluded from analysis.

The normative data based on the 0.5th, 1st, 2.5th, 5th, or 10th percentile cutoff values after correction of the inclination were separately constructed using data from the normal eyes[33,34] for mRNFL, GCIPL, and GCC, and sensitivity/specificity was calculated in the same manner as above.

Statistical Analysis

All statistical analyses were performed using (IBM SPSS Statistics 19; IBM Software, Japan, Tokyo) or the statistical programming language R (ver. 2.15.1; The R Foundation for Statistical Computing, Vienna, Austria).

Demographic data were compared between normal and OAG eyes by χ^2-test or Mann-Whitney U test because their normal distribution was rejected by the Kolmogorov-Smirnov test. Sensitivities and specificities were compared using McNemar's test. We used the AUC to evaluate the clinical usefulness of each condition, as suggested in a previous paper.[36] Comparison of multiple AUCs was carried out using DeLong's method.[37] Values of P less than 0.05 were considered significant.

RESULTS

Analyses Using mRNFL, GCC, and GCIPL

Finally, 104 eyes of 104 OAG patients among 181 initially enrolled OAG patients were enrolled. Sixteen of 181 eyes (8.8%) were excluded because the analysis area exceeded the data acquisition area, and the other eyes were excluded because of inadequate image data quality due to several factors,

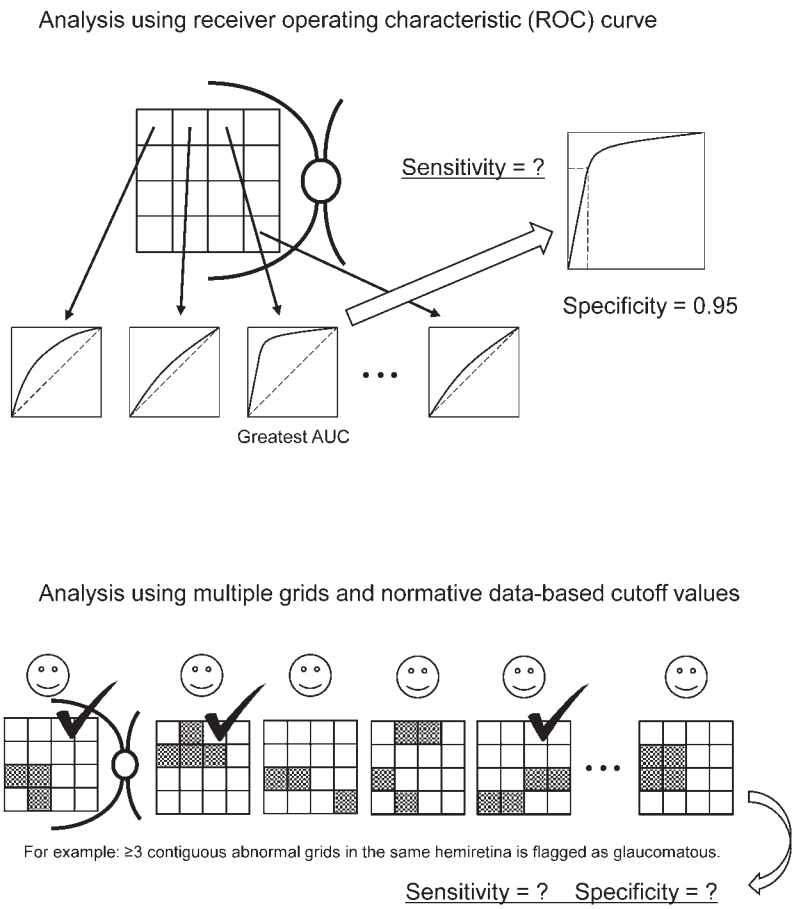

FIGURE 2. The procedure to evaluate capability of grid-wise analysis in the macular area. This schema shows a case of 4×4 grids as an example. In the ROC analysis, AUC of ROC curve is calculated for each grid and sensitivity was calculated when specificity was 0.95 in the grid with largest AUC. In the analysis using multiple grids and normative data–based cutoff values eyes, eyes with three or more (in this case, for example) contiguous abnormal grids in the same hemiretina is flagged as glaucomatous in both glaucomatous and normal subjects and sensitivity/specificity were calculated. The number of contiguous grids to judge as glaucomatous and cutoff values was varied.

including blinking, eye movements or obvious segmentation error.

Results of ROC analyses with specificity equal to 0.95 and those using variant normative data–based cutoff values yielding the highest sensitivity with specificity $\geq$ 0.95 under the given conditions are listed in Tables 2, 3, and 4 for the analyses of mRNFL, GCIPL, or GCC, respectively.

For macular RNFL, the highest sensitivity with a specificity $\geq$ 0.95 (sensitivity/specificity = 0.88/0.95) was obtained using three or four contiguous 8×8 grids outside the normative data–based 1st or 2.5th-percentile cutoff, respectively (Table 2).

For ganglion cell-inner plexiform layer, the highest sensitivity with specificity $\geq$ 0.95 (sensitivity/specificity = 0.80/0.96) was obtained using five contiguous 8×8 grids outside the 2.5th percentile cutoff (Table 3).

For ganglion cell complex, only analyses using 8×8 grids and normative data–based cutoff values yielded sensitivity $\geq$ 0.90 associated with specificity $\geq$ 0.95. That is, sensitivity/specificity equal to 0.90/0.96 was obtained using two or three contiguous 8×8 grids outside the 0.5th or 1st percentile cutoff, respectively (Table 4). Further, sensitivity/specificity equal to 0.88 or 0.89/0.95 to 0.98 was obtained under several conditions using 8×8 grids. The sensitivities/specificities obtained using the normative data-based 0.5th, 1st, 2.5th, 5th, and 10th percentile cutoff values for 8×8 grids of GCC are plotted in Figure 4.

Adoption of 8×8 grids yielded the highest sensitivity with specificity $\geq$ 0.95 for each macular inner layer, but only analyses using GCC attained sensitivity $\geq$ 0.90 with specificity $\geq$ 0.95 in the current subjects.

Comparison Between cpRNFL and Macular Inner Retinal Layer Thickness Measurements

Analyses using cpRNFL were performed in 86/104 OAG eyes and 77/104 normal eyes (Table 5), because cpRNFL measurement results satisfying the inclusion criteria were not obtained in 18 OAG and 27 normal eyes, probably because the cpRNFL measurements were performed after three repeated macular measurements.

Results of ROC analyses are shown in Table 6. The highest AUC (0.920) was obtained with inferotemporal 30° sector (seven o'clock in right eye orientation), which was not significantly different from those obtained with global average (0.892, $P = 0.32$), inferior 180° sector (0.883, $P = 0.11$), inferior 90° sector (0.891, $P = 0.18$). The highest sensitivity of 0.78 was obtained with specificity $\geq$ 0.95 using the 7 o'clock 30° sector. All sectors, including nerve fibers projecting the macular area, temporal 90° and 30° sectors located at 8, 9, or 10 o'clock, showed significantly smaller AUCs (0.662, 0.705, 0.564, and 0.626, respectively; $P < 0.01$) than that of global mean of cpRNFL (0.892).

Figure 3. (**a**) An example of the optic disc-fovea line and horizontal line. The angle "a" indicates inclination of the disc-fovea line, and positive angle indicates fovea is located below the horizontal line. (**b**) An example of location pattern of 8 × 8 grids in the 4.8 × 4.8-mm analysis area after compensation of the disc-fovea line inclination.

The analyses using variant normative data–based cutoff values yielding the highest sensitivity with specificity ≥ 0.95 under the given conditions are also listed in Table 6. The highest sensitivity with specificity ≥ 0.95 obtained using various normative data–based cutoff values was 0.63 using 180° sectors. The largest sensitivity/specificity of 0.76/0.94 was obtained using at least one 30° sector outside the first-percentile cutoff, though specificity did not reach to 0.95.

On the other hand, the highest sensitivity with specificity ≥ 0.95 obtained using mRNFL in the same eyes was 0.98 (sensitivity/specificity = 0.98/0.95) using three contiguous 8 × 8 grids outside the 2.5th-percentile cutoff, while those obtained using GCC and GCIPL in the same eyes were 0.93/0.96 using three contiguous 8 × 8 grids outside the first-percentile cutoff and 0.83/0.95 with three contiguous 8 × 8 grids outside the first-percentile cutoff, respectively.

The highest sensitivities of the mRNFL and GCC analyses were significantly higher than that of the cpRNFL analysis (0.98 vs. 0.78, $P = 0.001$ and 0.93 vs. 0.78, $P = 0.001$, respectively), while the same or a bit higher specificity of 0.95 or 0.96.

Table 2. Diagnostic Capability of mRNFL

	Analyses Based on ROC Curves in Each Single Area or Grid		Analyses Based on Various Normative Data–Based Cutoff Values in Single or Multiple Contiguous Grids	
Macular Area	Greatest–Smallest AUC (SE)	Sensitivity/Specificity (With 95% CI; Sensitivity at Fixed Specificity of 0.95)	Conditions*	Sensitivity/Specificity (With 95% CI; Highest Sensitivity at Specificity ≥ 0.95)
Whole area	0.944 (0.015)	0.76 (0.67–0.84)/0.95 (0.89–0.98)	5th percentile, the whole area	0.70 (0.60–0.79)/0.98 (0.93–1.00)
Upper or lower hemiretina	0.940 (0.016)–0.770 (0.032)	0.77 (0.68–0.85)/0.95 (0.89–0.98)	2.5th percentile, at least one hemiretina	0.80 (0.71–0.87)/0.98 (0.93–1.00)
4 × 4 grids	0.928 (0.018)–0.659 (0.038)	0.75 (0.66–0.83)/0.95 (0.89–0.98)	1st percentile, two contiguous grids	0.79 (0.70–0.86)/0.96 (0.90–0.99)
8 × 8 grids	0.919 (0.019)–0.513 (0.040)	0.72 (0.62–0.80)/0.95 (0.89–0.98)	1st percentile, three contiguous grids	0.88 (0.81–0.94)/0.95 (0.89–0.98)
			2.5th percentile, four contiguous grids	0.88 (0.81–0.94)/0.95 (0.89–0.98)

CI, confidence interval.

* Conditions where the eyes were flagged as glaucomatous with respect to the normative data–based cutoff values and numbers of abnormal grids.

Table 3. Diagnostic Capability of Macular GCIPL

	Analyses Based on ROC Curves in Each Single Area or Grid		Analyses Based on Variant Normative Data–Based Cutoff Values in Single or Multiple Contiguous Grids	
Macular Area	**Greatest–Smallest AUC (SE)**	**Sensitivity/Specificity (With 95% CI; Sensitivity at Fixed Specificity of 0.95)**	**Conditions***	**Sensitivity/Specificity (With 95% CI; Highest Sensitivity at Specificity ≥ 0.95)**
Whole area	0.912 (0.019)	0.47 (0.37–0.57)/0.95 (0.89–0.98)	2.5th percentile, the whole area	0.42 (0.33–0.52)/0.98 (0.93–1.00)
Upper or lower hemiretina	0.869 (0.025)–0.695 (0.037)	0.55 (0.45–0.65)/0.95 (0.89–0.98)	2.5th percentile, at least one hemiretina	0.50 (0.40–0.60)/0.96 (0.90–0.99)
4 × 4 grids	0.884 (0.023)–0.580 (0.041)	0.56 (0.46-0.66)/0.95 (0.89–0.98)	0.5th percentile, at least one hemiretina	0.75 (0.66–0.83)/0.96 (0.90–0.99)
8 × 8 grids	0.898 (0.022)–0.545 (0.041)	0.58 (0.48–0.67)/0.95 (0.89–0.98)	2.5th percentile, five contiguous grids	0.80 (0.71–0.87)/0.96 (0.90–0.99)

* Conditions where the eyes were flagged as glaucomatous with respect to the normative data–based cutoff values and numbers of abnormal grids.

Table 4. Diagnostic Capability of Macular GCC

	Analyses Based on ROC Curves in Each Single Area or Grid		Analyses Based on Variant Normative Data–Based Cutoff Values in Single or Multiple Contiguous Grids	
Macular Area	**Greatest–Smallest AUC (SE)**	**Sensitivity/Specificity (With 95% CI; Sensitivity at Fixed Specificity of 0.95)**	**Conditions***	**Sensitivity/Specificity (With 95% CI; Highest Sensitivity at Specificity ≥ 0.95)**
Whole area	0.912 (0.019)	0.71 (0.61–0.80)/0.95 (0.89–0.98)	5th percentile, the whole area	0.62 (0.51–0.71)/0.96 (0.90–0.99)
Upper or lower hemiretina	0.931 (0.018)–0.754 (0.034)	0.69 (0.59–0.78)/0.95 (0.89–0.98)	2.5th percentile, at least 1 hemiretina	0.74 (0.64–0.82)/0.99 (0.95–1.00)
4 × 4 grids	0.934 (0.017)–0.650 (0.038)	0.76 (0.67–0.84)/0.95 (0.89–0.98)	1st percentile, two contiguous grids	0.86 (0.77–0.92)/0.97 (0.92–0.99)
8 × 8 grids	0.936 (0.017)–0.595 (0.040)	0.78 (0.69–0.85)/0.95 (0.89–0.98)	0.5th percentile, two contiguous grids	0.90 (0.83–0.95)/0.96 (0.90–0.99)
			1st percentile, three contiguous grids	0.90 (0.83–0.95)/0.96 (0.90–0.99)

* Conditions where the eyes were flagged as glaucomatous in respect of the normative data-based cutoff values and numbers of abnormal grids.

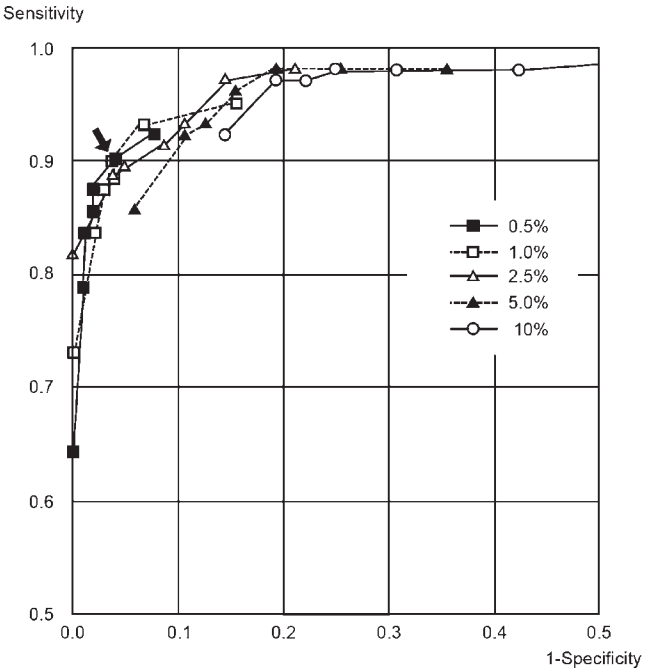

Figure 4. Sensitivity and specificity plots using the 8 × 8 grids of GCC with various normative data–based cutoff values (0.5th, 1st, 2.5th, 5th, and 10th percentile) and number of abnormal contiguous grids (1–7) to be diagnosed with glaucoma; 0.5%, 1.0%, 2.5%, 5.0%, and 10% indicate normative data–based cutoff values of 0.5th, 1st, 2.5th, 5th, and 10th percentile, respectively. The *black arrow* indicates the conditions of sensitivity equal to 0.90 and specificity equal to 0.96; 0.5th percentile, two contiguous grids and 1st percentile, three contiguous grids. See also Table 4.

Effects of Compensation of Inclination of Disc-Fovea Line

The calculated inclination was 7.8° ± 3.2° (mean ± SD) in normal eyes and 8.0° ± 2.7° in glaucoma eyes ($n = 104$ each), with no significant difference between them ($P = 0.65$).

In some eyes, the peripheral 8 × 8 grids exceeded the data acquisition area edge after compensating for the inclination and were excluded from analysis. Valid data in a 4.8 × 4.8-mm macular area with and without compensation for inclination of disc-fovea line were obtained in 89 normal and 88 OAG eyes (Table 7). Performance of the optimum or suboptimum condition in detecting early-stage glaucoma was compared between with and without correction of inclination, but diagnostic capability was not significantly improved under any conditions. Representative results with the highest or the second highest sum of sensitivity and specificity are summarized in Table 8. Almost identical sensitivity and specificity, approximately 0.95, were obtained using reconstructed 8 × 8 grids of GCC or mRNFL in the 4.8 × 4.8-mm area and reconstructed normal data–based cutoff values after compensation of inclination of disc-fovea line.

Discussion

Spectral-domain OCT allows for efficient analysis of the intraretinal layers in the macular region, and most previous studies report that GCC and GCIPL thicknesses yields reasonably reproducible measurements[38–40] and are effective for diagnosing glaucoma, similar to cpRNFL analysis.[20,24–26,41–44] In glaucoma, especially early-stage glaucoma, retinal thickness decreases in localized areas in the macular region[45,46] and analyzing subdivided macular regions should improve sensitivity.[28] Therefore, we compared the results of grid-wise analyses of mRNFL, GCIPL, and GCC thickness among 1 × 2, 4 × 4, and 8 × 8 grids.

Table 5. Characteristics of Subjects Adopted for Comparison Between Macular and Circumpapillary Measurement

Glaucomatous Damage	Normal	Early Stage
Number of subjects, eyes	77	86
Women/men	42/35	42/44
Age, y	56.9 ± 11.2	58.3 ± 10.7
Refraction, D	−0.97 ± 1.30	−1.40 ± 2.17
Mean deviation, dB*	−0.06 ± 1.21	−1.80 ± 1.92

Refraction indicates spherical equivalent of the subject eye. Mean deviation indicates mean deviation of a central 24-2 test program of Humphrey Field Analyzer. Intergroup difference was significant at *$P <$ 0.001, Mann-Whitney U test.

Sensitivity at specificity equal to 0.95 determined on ROC curve with the largest AUC was higher than that obtained using various normative data–based cutoff values in the whole macula. On the other hand, adoption of ≥2 grids from multiple grids and certain normative data–based cutoff values yielded higher sensitivity with similar specificity, while greater grid size and higher number of contiguous grids flagged as abnormal tended to result in lower sensitivity and higher specificity. The criteria was based on 2 or more 8 × 8 grids outside normative data–based cutoff values, in which grid size was 2.4° × 2.4° roughly corresponding to the grid size of the HFA 10-2 program, showed better diagnostic performance than the others. Even smaller grid sizes might give better results. Because the grid size of the HFA 10-2 program is 2.0° × 2.0°, however, OCT measurement results from retinal areas smaller than 2.0° × 2.0° may not be practical in diagnosing glaucoma based on the structure-function relationship using conventional VF testing.

Although there was no significant difference in the highest sensitivity with specificity ≥ 0.95 obtained using mRNFL and GCC thickness–based criteria, only the GCC thickness–based criteria yielded sensitivity ≥ 0.90 for discriminating early-stage OAG eyes with a mean MD of −1.8 dB from normal eyes. Combination of GCIPL and mRNFL, GCC, had a significantly higher sensitivity than GCIPL (0.90 and 0.80, respectively, $P =$ 0. 013) in the subjects of this study in early-stage of the disease.

According to the cpRNFL analysis, largest AUC was obtained with inferior sectors rather than temporal sectors. On the other hand, a global average of cpRNFL also showed no smaller AUC than those though the subjects were limited to the early-stage glaucoma. Those results may suggest a limitation of circle-wise sector analysis of cpRNFL in diagnosis of early-stage glaucoma.[47]

To our knowledge, SD-OCT–based diagnostic performance with sensitivity ≥ 0.90 and specificity ≥ 0.95 is rarely reported, only in eyes of moderate glaucoma damage (MD of −8.99 ± 8.16 dB[10] or MD ranged from −15.87 to +0.07 dB with median of −4.58 dB[48] or eyes with early-stage but manifest glaucomatous visual field defects (MD of −2.5 ± 1.8 dB) using grid-wise analyses of peripapillary retinal nerve fiber layer thickness.[47] Furthermore, mRNFL or GCC thickness-based criteria showed significantly better diagnostic performance than the best clock-hour cpRNFL-based criterion in the same eyes. These results adopting normative data-based cutoff values are readily applicable to clinical practice.

Inclination of the disc-fovea line might be a critical issue in grid-wise analysis of the macula using SD-OCT.[13] The present results, however, suggested that compensation of the inclination barely affected diagnostic performance. This finding might

Investigative Ophthalmology & Visual Science

TABLE 6. Diagnostic Capability of cpRNFL and Comparison With mRNFL and GCC

		Analyses Based on ROC Curves in Each Single Sector		Analyses Based on Variant Normative Data–Based Cutoff Values in Single or Multiple Contiguous Sectors/Grids	
	Sector Width/ Grid Pattern	Greatest–Smallest AUC (SE)	Sensitivity/Specificity (With 95% CI; Sensitivity at Fixed Specificity of 0.95)	Conditions*	Sensitivity/Specificity (With 95% CI; Highest Sensitivity at Specificity $\geq$ 0.95)
cpRNFL	360°	0.892 (0.025)	0.57 (0.46-0.68)/0.95 (0.87–0.99)	5th percentile, the whole circle	0.48 (0.37–0.59)/0.95 (0.87–0.99)
	180°	0.883 (0.026)–0.822 (0.032)	0.63 (0.52-0.73)/0.95 (0.87–0.99)	2.5th percentile, at least 1 half	0.63 (0.52–0.73)/0.95 (0.87–0.99)
	90°	0.891 (0.024)–0.662 (0.042)	0.64 (0.53-0.74)/0.95 (0.87–0.99)	1st percentile, at least one sector	0.56 (0.45–0.67)/0.95 (0.87–0.99)
	30°	0.920 (0.022)–0.564 (0.045)	0.78 (0.68–86)/0.95 (0.87–0.99)	2.5th percentile, two contiguous sectors	0.45 (0.35–0.56)/0.96 (0.89–0.99)
mRNFL, GCC	8 × 8 grids			2.5th percentile, three contiguous grids	0.98 (0.92–1.00)/0.95 (0.87–0.99)
	8 × 8 grids			1st percentile, three contiguous grids	0.93 (0.85–0.97)/0.96 (0.89–99)

Analyses were performed in the subjects listed in Table 5.
* Conditions where the eyes were flagged as glaucomatous with respect to the normative data-based cutoff values and numbers of abnormal sectors or grids.

TABLE 7. Characteristics of the Subjects Adopted for Comparison Between Without and With Compensation of the Inclination of the Disc-Fovea Line

Glaucomatous Damage	Normal	Early-Stage
Number of subjects, eyes	89	88
Women/men	43/46	46/42
Age, y	56.6 ± 11.3	57.7 ± 10.2
Refraction, D	−1.14 ± 1.30	−1.59 ± 2.15
Inclination angle, degrees	7.6 ± 2.8	8.0 ± 2.5
Mean deviation, dB*	−0.09 ± 1.20	−1.74 ± 1.87

Refraction indicates spherical equivalent of the subject eye. Inclination angle indicates the angle between the disc-fovea line and the horizontal line, and positive angle indicates fovea is located below the horizontal line. Mean deviation indicates mean deviation of a central 24-2 test program of Humphrey Field Analyzer. Intergroup difference was significant at *$P < 0.001$, Mann-Whitney U test.

be due to: 1) the relatively small degree of inclination (mean 7.6° or 8.0°) and insufficient lateral resolution of the SD-OCT system; 2) ~15% of the current subject eyes could not be included because the most peripheral grids exceeded the data acquisition area edge when the grids were reconfigured in parallel with the disc-fovea line. Thus, the number of subject eyes might not be sufficient; 3) the stage of OAG of the current subjects (mean MD −1.8 dB) might not be adequate to detect the advantage of correcting the inclination. Correction of the inclination might be advantageous if asymmetry between the upper and lower hemimacula is incorporated in the diagnostic criteria.[49,50]

To elucidate the effect of the angle between disc-fovea line and the horizontal line on glaucoma diagnosis, diagnostic capability was compared between subgroups of the subjects divided by the degree of the angle without reconstruction of the grid. The subject eyes were divided into three subgroups: those with small (<6.65°), average (6.65°–9.35°), and large (>9.35°) angle each consisted with 22 to 41 normal or glaucomatous eyes which were determined by (mean ± 1/2 SD) of the angle in the all subject eyes of this study. In the macular analyses, sensitivity and specificity were recalculated in those subgroups separately using three or four contiguous 8 × 8 grids of mRNFL outside the normative data–based 1st or 2.5th percentile cutoff, respectively, and two or three contiguous 8 × 8 grids of GCC outside the 0.5th or 1st percentile cutoff, respectively, which showed the highest sensitivity/specificity (0.88/0.95 for mRNFL and 0.90/0.96 for GCC) in the whole subjects. Specificity remained ≥ 0.95 in the all subgroups with small or large angle except the method based on three contiguous GCC grids outside the 1st percentile cutoff (0.93). Sensitivity decreased to 0.89 or 0.77 in the subgroup with large or small angle in the methods using mRNFL and decreased 0.77 to 0.82 in the subgroup with small angle in the methods using GCC. In the method using cpRNFL, AUC of ROC was recalculated in those subgroups. The highest AUC (0.912, 0.907, and 0.938) was obtained with inferotemporal 30° sector (7 o'clock in right eye) in the subgroups with small, average, and large angle and that was followed by global average, inferior 90°, or 180° sector just similar to the case with all subjects. Those results suggest the inclination of disc-fovea line has little effect on specificity in normal eyes in the grid-wise macular analysis and sector-wise cpRNFL analysis using at least 30° or wider sectors. Detection of glaucomatous damage in the macula may be disturbed by the angle and there is a possibility to improve it by an approach other than reconfiguration of the grids.

The present study has several limitations. The criteria used were not compared and verified in a separate group of normal

Table 8. Comparison of Sensitivity/Specificity for Glaucoma Detection With and Without Compensation of the Inclination of the Disc-Fovea Line

Conditions (8 × 8 grids)	Macular Inner Retinal Layer	Compensation, −	Compensation, +
Three contiguous grids outside the 0.5th percentile cutoff	GCC	0.94/0.94	0.94/0.94
Three contiguous grids outside the 1st percentile cutoff	GCC	0.92/0.97	0.91/0.96
Three contiguous grids outside the 1st percentile cutoff	mRNFL	0.93/0.94	0.93/0.94
Three contiguous grids outside the 2.5th percentile cutoff	mRNFL	0.97/0.96	0.95/0.94

Values indicate sensitivity/specificity. Compensation (–) indicates no compensation of inclination of disc-fovea line and compensation (+) indicates compensation of inclination of disc-fovea line.

and glaucoma eyes, and thus the clinical usefulness of the current optimum criterion requires further confirmation. Most of the current OAG patients had untreated normal IOP (normal tension glaucoma). Differences in the VFD pattern (i.e., differences in GCL damage distribution), between OAG patients with normal and elevated IOP, have been reported.[51] Thus, the current optimum criterion may not be optimum in a group of OAG patients with elevated IOP. Comparison of the diagnostic capability between cpRNFL and macular inner retinal layers or effects of compensation of the inclination could only be studied in ~85% of the subjects. Although no significant difference was detected in the degree of glaucomatous damage or ocular and systemic factors between those included and not included (Tables 1, 5, and 7), this somewhat decreased the power of detection. Longitudinal and horizontal density of sampling points of the OCT apparatus was not equal (128 × 512) and its optimized rearrangement might have a significant effect on the results.

In summary, the 5.5 × 5.5-mm macular area was subdivided in a grid-wise manner and measured by SD-OCT in up to 8 × 8 grids, and diagnostic capability for early-stage glaucoma (mean MD −1.8 dB) was compared based on ROC analyses and various normative data–based cutoff values for mRNFL, GCIPL, and GCC thickness in each grid and the number of abnormal grids. The 8 × 8 grid-GCC analysis yielded a sensitivity $\geq$ 0.90 and specificity $\geq$ 0.95 under two conditions, that is, two contiguous grids outside the 0.5th percentile cutoff or three contiguous grids outside first-percentile cutoff of normative data. Compensation of physiological inclination of disc-fovea line did not significantly affect diagnostic capability in the current subjects.

Acknowledgments

Supported by grant-in-aid for Scientific Research by the Ministry of Health, Labor and Welfare of Japan (H18-Sensory-General-001) and Topcon, Inc. (Tokyo, Japan). None of the authors has a proprietary interest in any products described in the article.

Disclosure: **C. Mayama**, Topcon, Inc. (R); **H. Saito**, Topcon, Inc. (R); **H. Hirasawa**, Topcon, Inc. (R); **A. Tomidokoro**, Topcon, Inc. (R); **M. Araie**, Topcon, Inc. (F, C, S); **A. Iwase**, Topcon, Inc. (R); **S. Ohkubo**, Topcon, Inc. (R); **K. Sugiyama**, Topcon, Inc. (R); **M. Hangai**, Topcon, Inc. (R); **N. Yoshimura**, Topcon, Inc. (F, C, S)

References

1. Hoh ST, Greenfield DS, Mistlberger A, Liebmann JM, Ishikawa H, Ritch R. Optical coherence tomography and scanning laser polarimetry in normal, ocular hypertensive, and glaucomatous eyes. *Am J Ophthalmol*. 2000;129:129–135.
2. Bowd C, Zangwill LM, Berry CC, et al. Detecting early glaucoma by assessment of retinal nerve fiber layer thickness and visual function. *Invest Ophthalmol Vis Sci*. 2001;42:1993–2003.
3. Leung CK, Chan WM, Chong KK, et al. Comparative study of retinal nerve fiber layer measurement by StratusOCT and GDx VCC. I: correlation analysis in glaucoma. *Invest Ophthalmol Vis Sci*. 2005;46:3214–3220.
4. Deleon-Ortega JE, Arthur SN, McGwin G Jr, Xie A, Monheit BE, Girkin CA. Discrimination between glaucomatous and non-glaucomatous eyes using quantitative imaging devices and subjective optic nerve head assessment. *Invest Ophthalmol Vis Sci*. 2006;47:3374–3380.
5. Bowd C, Zangwill LM, Medeiros FA, et al. Structure-function relationships using confocal scanning laser ophthalmoscopy, optical coherence tomography, and scanning laser polarimetry. *Invest Ophthalmol Vis Sci*. 2006;47:2889–2895.
6. Hong S, Ahn H, Ha SJ, Yeom HY, Seong GJ, Hong YJ. Early glaucoma detection using the Humphrey Matrix Perimeter, GDx VCC, Stratus OCT, and retinal nerve fiber layer photography. *Ophthalmology*. 2007;114:210–215.
7. Sehi M, Ume S, Greenfield DS. Scanning laser polarimetry with enhanced corneal compensation and optical coherence tomography in normal and glaucomatous eyes. *Invest Ophthalmol Vis Sci*. 2007;48:2099–2104.
8. Sung KR, Kim DY, Park SB, Kook MS. Comparison of retinal nerve fiber layer thickness measured by Cirrus HD and Stratus optical coherence tomography. *Ophthalmology*. 2009;116:1264–1270.
9. Chang RT, Knight OJ, Feuer WJ, Budenz DL. Sensitivity and specificity of time-domain versus spectral-domain optical coherence tomography in diagnosing early to moderate glaucoma. *Ophthalmology*. 2009;116:2294–2299.
10. Leung CK, Lam S, Weinreb RN, et al. Retinal nerve fiber layer imaging with spectral-domain optical coherence tomography: analysis of the retinal nerve fiber layer map for glaucoma detection. *Ophthalmology*. 2010;117:1684–1691.
11. Park SB, Sung KR, Kang SY, Kim KR, Kook MS. Comparison of glaucoma diagnostic Capabilities of Cirrus HD and Stratus optical coherence tomography. *Arch Ophthalmol*. 2009;127:1603–1609.
12. Sehi M, Grewal DS, Sheets CW, Greenfield DS. Diagnostic ability of Fourier-domain vs time-domain optical coherence tomography for glaucoma detection. *Am J Ophthalmol*. 2009;148:597–605.
13. Chauhan B, Burgoyne CF. From clinical examination of the optic disc to clinical assessment of the optic nerve head: a paradigm change. *Am J Ophthalmol*. 2013;156:218–227. 2009;148:597–605.
14. Curcio CA, Allen KA. Topography of ganglion cells in human retina. *J Comp Neurol*. 1990;300:5–25.
15. Tan O, Li G, Lu AT, Varma R, Huang D. Mapping of macular substructures with optical coherence tomography for glaucoma diagnosis. *Ophthalmology*. 2008;115:949–956.
16. Yang Q, Reisman CA, Wang Z, et al. Automated layer segmentation of macular OCT images using dual scale gradient information. *Opt Express*. 2010;18:21293–21307.
17. Mwanza JD, Oakley D, Budanz DL, Chang RT, Knight OJ, Feuer WJ. Macular ganglion cell-inner plexiform layer: automated detection and thickness reproducibility with spectral domain-optical coherence tomography in glaucoma. *Invest Ophthalmol Vis Sci*. 2011;52:8323–8329.

18. Tan O, Chopra V, Lu AT, et al. Detection of macular ganglion cell loss in glaucoma by Fourier-domain optical coherence tomography. *Ophthalmology*. 2009;116:2305–2314.
19. Mori S, Hangai M, Sakamoto A, Yoshimura N. Spectral-domain optical coherence tomography measurement of macular volume for diagnosing glaucoma. *J Glaucoma*. 2010;19:528–534.
20. Garas A, Vargha P, Hollo G. Diagnostic accuracy of nerve fibre layer, macular thickness and optic disc measurements made with the RTVue-100 optical coherence tomograph to detect glaucoma. *Eye*. 2011;25:57–65.
21. Na JH, Kook MS, Lee Y, Yu SJ, Choi J. Detection of macular and circumpapillary structural loss in normal hemifield areas of glaucomatous eyes with localized visual field defects using spectral-domain optical coherence tomography. *Graefes Arch Clin Exp Ophthalmol*. 2012;250:595–602.
22. Takagi ST, Kita Y, Yagi F, Tomita G. Macular retinal ganglion cell complex damage in the apparently normal visual field of glaucomatous eyes with hemifield defects. *J Glaucoma*. 2012; 21:318–325.
23. Kim NR, Lee ES, Seong GJ, Kim JH, An HG, Kim CY. Structure-function relationship and diagnostic value of macular ganglion cell complex measurement using Fourier-domain OCT in glaucoma. *Invest Ophthalmol Vis Sci*. 2010;51:4646–4651.
24. Seong M, Sung KR, Choi EH, et al. Macular and peripapillary retinal nerve fiber layer measurements by spectral domain optical coherence tomography in normal-tension glaucoma. *Invest Ophthalmol Vis Sci*. 2010;51:1446–1452.
25. Mwanza JC, Durbin MK, Budenz DL, et al. Glaucoma diagnostic accuracy of ganglion cell-inner plexiform layer thickness: comparison with nerve fiber layer and optic nerve head. *Ophthalmology*. 2012;119:1151–1158.
26. Kotowski J, Folio LS, Wollstein G, et al. Glaucoma discrimination of segmented cirrus spectral domain optical coherence tomography (SD-OCT) macular scans. *Br J Ophthalmol*. 2012; 96:1420–1425.
27. Akashi A, Kanamori A, Nakamura M, Fujihara M, Yamada Y, Negi A. Comparative assessment of Cirrus, RTVue and 3D-OCT to diagnose glaucoma. *Invest Ophthalmol Vis Sci*. 2013;45: 4478–4484.
28. Kanamori A, Naka M, Akashi A, Fujihara M, Yamada Y, Nakamura M. Cluster analysis of grid pattern display in macular parameters using optical coherence tomography for glaucoma diagnosis. *Invest Ophthalmol Vis Sci*. 2013;54: 6401–6408.
29. Hood DC, Raza AS, Gustavo C, et al. Initial arcuate defects within the central 10 degrees in glaucoma. *Invest Ophthalmol Vis Sci*. 2011;52:940–946.
30. Anderson DR, Patella VM. *Automated Static Perimetry*. 2nd ed. St. Louis, MO: Mosby; 1999.
31. Littman H. Zur Bestimmung der wahren Größe eines Objektes auf dem Hintergrund des lebenden Auges. *Klin Monatsbl Augenheilkd*. 1982;180:286–289.
32. Littman H. Zur Bestimmung der wahren Größe eines Objektes auf dem Hintergrund eines lebenden Auges. *Klin Monatsbl Augenheilkd*. 1988;192:66–67.
33. Ooto S, Hangai M, Sakamoto A, et al. Three-dimensional profile of macular retinal thickness in normal Japanese eyes. *Invest Ophthalmol Vis Sci*. 2010;51:465–473.
34. Ooto S, Hangai M, Tomidokoro A, et al. Effects of age, sex and axial length on the three-dimensional profile of normal macular layer structures. *Invest Ophthalmol Vis Sci*. 2011; 52:8769–8779.
35. Hirasawa H, Tomidokoro A, Araie M, et al. Peripapillary retinal nerve fiber layer thickness determined by spectral-domain optical coherence tomography in ophthalmologically normal eyes. *Arch Ophthalmol*. 2010;128:1420–1426.
36. Demšar J. Statistical comparisons of classifiers over multiple data sets. *J Mach Learn Res*. 2006;7:1–30.
37. DeLong ER, DeLong DM, Clarke-Pearson DL. Comparing the areas under two or more correlated receiver operating characteristic curves: a nonparametric approach. *Biometrics*. 1988;44:837–845.
38. Garas A, Vargha P, Hollo G. Reproducibility of retinal nerve fiber layer and macular thickness measurement with the RTVue-100 optical coherence tomograph. *Ophthalmology*. 2010;117:738–746.
39. Mwanza JC, Oakley JD, Budenz DL, Chang RT, Knight OJ, Feuer WJ. Macular ganglion cell-inner plexiform layer: automated detection and thickness reproducibility with spectral domain-optical coherence tomography in glaucoma. *Invest Ophthalmol Vis Sci*. 2011;52:8323–8329.
40. Hirasawa H, Araie M, Tomidokoro A, et al. Reproducibility of thickness measurement of macular inner retinal layers using SD-OCT with or without correction of ocular rotation. *Invest Ophthalmol Vis Sci*. 2013;54:2562–2570.
41. Kim NR, Lee ES, Seong GJ, et al. Comparing the ganglion cell complex and retinal nerve fiber layer measurements by Fourier domain OCT to detect glaucoma in high myopia. *Br J Ophthalmol*. 2011;95:1115–1121.
42. Schulze A, Lamparter J, Pfeiffer N, Berisha F, Schmidtmann I, Hoffmann EM. Diagnostic ability of retinal ganglion cell complex, retinal nerve fiber layer, and optic nerve head measurements by Fourier-domain optical coherence tomography. *Graefes Arch Clin Exp Ophthalmol*. 2011;249:1039–1045.
43. Rao HL, Babu JG, Addepalli UK, Senthil S, Garudadri CS. Retinal nerve fiber layer and macular inner retina measurements by spectral domain optical coherence tomograph in Indian eyes with early glaucoma. *Eye*. 2012;26:133–139.
44. Na JH, Sung KR, Baek S, Sun JH, Lee Y. Macular retinal nerve fiber layer thickness: which is more helpful in the diagnosis of glaucoma? *Invest Ophthalmol Vis Sci*. 2011;52:8094–8101.
45. Raza AS, Cho J, de Moraes CGV, et al. Retinal ganglion cell layer thickness and local visual field sensitivity in glaucoma. *Arch Ophthalmol*. 2011;129:1529–1536.
46. Morooka S, Hangai M, Nukada M, et al. Wide 3-dimensional macular ganglion cell complex imaging with spectral-domain optical coherence tomography in glaucoma. *Invest Ophthalmol Vis Sci*. 2012;53:4805–4812.
47. Mayama C, Saito H, Hirasaya H, et al. Circle- and grid-wise analyses of peripapillary nerve fiber layer by spectral domain optical coherence tomography in early-stage glaucoma. *Invest Ophthalmol Vis Sci*. 2013;54:4519–4526.
48. Bengtsson B, Andersson A, Heijl A. Performance of time-domain and spectral-domain optical coherence tomography for glaucoma screening. *Acta Ophthalmol*. 2012;90:310–315.
49. Asrani S, Rosdahl JA, Allingham RR. Novel software strategy for glaucoma diagnosis. Asymmetry analysis of retinal thickness. *Arch Ophthalmol*. 2011;129:1205–1211.
50. Um TW, Sung KR, Wollstein G, Yun SC, Na JH, Schuman JS. Asymmetry in hemifield macular thickness as an early indicator of glaucomatous change. *Invest Ophthalmol Vis Sci*. 2012;53:1139–1144.
51. Araie M. Pattern of visual field defect in normal-tension and high-tension glaucoma. *Curr Opin Ophthalmol*. 1995;6:36–45.

Investigative Ophthalmology & Visual Science